Available online at www.sciencedirect.com
ScienceDirect
Journal of Catalysis 254 (2008) 190–197
JOURNAL OF CATALYSIS
www.elsevier.com/locate/jcat

Influence of water on the activity and stability of activated Mg–Al hydrotalcites for the transesterification of tributyrin with methanol

Yuanzhou Xi, Robert J. Davis *

Department of Chemical Engineering, University of Virginia, 102 Engineers' Way, P.O. Box 400741, Charlottesville, VA 22904-4741, USA

Received 14 September 2007; revised 10 December 2007; accepted 16 December 2007

Available online 25 January 2008

Abstract

Magnesium–aluminum hydrotalcite with a Mg/Al molar ratio of 4 was synthesized by a coprecipitation method. Thermally-decomposed and rehydrated Mg–Al hydrotalcites were used to catalyze the transesterification of tributyrin, a model triglyceride, with methanol (tributyrin:methanol molar ratio 1:30) at 333 K to produce methyl butyrate, monobutyrin, dibutyrin, and glycerol. The pseudo first order rate constants of a three step reaction sequence for tributyrin transesterification were determined by fitting a kinetic model to the experimental data. Although decomposed and rehydrated Mg–Al hydrotalcite was one order of magnitude more active than decomposed Mg–Al hydrotalcite based on surface area measured by N_2 adsorption, the activity correlated well to the CO_2 adsorption capacity. The most active rehydrated samples also deactivated faster, presumably because butyric acid produced by hydrolysis of ester with adsorbed water reacted with the base sites. The areal rate and CO_2 adsorption capacity of decomposed-rehydrated Mg–Al hydrotalcite decreased as the interlayer water was removed by heating.

Keywords: Hydrotalcite; Biodiesel; Transesterification; Decomposition; Rehydration; Brønsted base site; Lewis base site; Interlayer water; Kinetics; CO_2 adsorption

1. Introduction

Biodiesel is an attractive biorenewable alternative to petroleum-based transportation fuels. Common feedstocks for the production of biodiesel include triglycerides found in vegetable oils and animal fats. These triglycerides can undergo catalytic transesterification with methanol or ethanol to form monoalkyl esters commonly known as biodiesel [1–4]. Since biodiesel is free of sulfur and aromatic species and contributes much less to global warming than fossil fuels, it is considered to be an environmentally-friendly fuel alternative [1,4,5]. Moreover biodiesel can be added to low sulfur petroleum-derived diesel to improve its lubricity [1]. Classically, homogeneous base catalysts such as alkali metal hydroxide or methoxide are often used to catalyze the transesterification reaction for biodiesel production, however separation of the homogeneous catalyst from the reaction solution is difficult [6]. Heterogeneous catalysts would be preferred since they can be easily separated and reused.

Metals, metal oxides and zeolites have been studied for the catalytic transesterification reactions [7–10]. In particular, Mg–Al hydrotalcite is a potentially interesting catalyst for transesterification since it is recognized as an anion exchanger, an adsorbent and a solid base catalyst [11].

Hydrotalcite with a general formula of $[Mg_{(1-x)}Al_x(OH)_2]^{x+}(CO_3)_{x/2}{}^{2-}\cdot nH_2O$ is a class of double layered anionic clay having brucite-like $Mg(OH)_2$ layers, where magnesium cations are octahedrally-coordinated with hydroxyl ions and share edges to form brucite-like layers. When a magnesium cation is replaced by an aluminum cation, a positive charge is generated in the layer, which is balanced by an anion such as carbonate or hydroxyl located between the layers. Water molecules can also be present in the interlayer space. Decomposition of Mg–Al hydrotalcite yields a high surface area Mg–Al mixed oxide, which presumably exposes strong Lewis base sites [12–14]. The basic properties of these sites depend on the Mg–Al ratio in the precursor hydrotalcite [11,13,15].

* Corresponding author. Fax: +1 434 982 2658.
E-mail addresses: yx8f@virginia.edu (Y. Xi), rjd4f@virginia.edu (R.J. Davis).

0021-9517/$ – see front matter
doi:10.1016/j.jcat.2007.12.008

Interestingly, the reconstruction of decomposed Mg–Al hydrotalcite by rehydration at room temperature has been reported to enhance the catalytic activity [16]. During the rehydration, the brucite-like layers are reformed and the charge-compensating carbonate anions are replaced by hydroxyl anions, thus forming Brønsted base sites. The decomposed-rehydrated Mg–Al hydrotalcite with Brønsted base sites exhibits higher catalytic activity than the decomposed Mg–Al hydrotalcite with Lewis base sites for the aldol condensation of benzaldehyde with acetone [16], aldol condensation of citral with ketones [17], self-aldolization of acetone [17], Michael addition reactions [18], and the transesterification of oleic acid methyl ester with glycerol [12].

Recently, Cantrell et al. showed that thermally activated Mg–Al hydrotalcites with various Mg–Al ratios are effective catalysts for transesterification of tributyrin with methanol, with catalytic activity increasing as the Mg content in the Mg–Al hydrotalcite increased [19].

In this work, Mg–Al hydrotalcite with Mg/Al molar ratio of 4 was prepared as the catalyst precursor. The catalytic activity of decomposed and rehydrated Mg–Al hydrotalcites was then tested in the transesterification of tributyrin with methanol. The catalyst structure and CO_2 adsorption capacity were evaluated as a function of pretreatment temperature and then related to the observed activity.

2. Experimental methods

2.1. Catalyst preparation

A coprecipitation method was used to synthesize Mg–Al hydrotalcite. First, an aqueous solution (200 ml) containing 0.24 mol $Mg(NO_3)_2{\cdot}6H_2O$ (Acros, 98%) and 0.06 mol $Al(NO_3)_3{\cdot}9H_2O$ (Aldrich, 98%) and another aqueous solution (200 ml) containing 0.468 mol NaOH (Mallinckrodt, 99%) and 0.12 mol Na_2CO_3 (Aldrich, 99.95%) were added dropwise into 50 ml of distilled deionized (DDI) water at 338 K and stirred for 22 h at 338 K. The mixture was filtered and the recovered precipitate was washed thoroughly with DDI water (about 340 K). The resulting hydrotalcite was dried at 338 K in air for 24 h, ground into powder, and sieved between 0.038 and 0.075 mm to give the catalyst precursor, denoted as HT.

The decomposed Mg–Al hydrotalcite, denoted as HT-d, was prepared by heating HT to 723 K under 100 $cm^3\,min^{-1}$ of flowing N_2 (Messer, 99.999%). The temperature was raised to 723 K at a rate of 10 $K\,min^{-1}$ and maintained at 723 K for 8 h before cooling to room temperature. The decomposed-rehydrated Mg–Al hydrotalcite, denoted as HT-d-r, was prepared by flowing 100 $cm^3\,min^{-1}$ of wet N_2 (2.6 vol% H_2O, by bubbling N_2 through 200 ml of aqueous solution containing 9.1% NaCl) through HT-d for 24 h at room temperature. After rehydration, the HT-d-r sample was progressively heated to remove water in stages. The thermal treatment occurred at 333, 373, 423, or 473 K after heating at a rate of 5 $K\,min^{-1}$ in 100 $cm^3\,min^{-1}$ of flowing N_2 and maintaining temperature for 1 h prior to cooling to room temperature. The HT-d-r was also decomposed by ramping the temperature to 723 K at 5 $K\,min^{-1}$ in 100 $cm^3\,min^{-1}$ of flowing N_2, holding for 1 h and cooling to room temperature. These catalysts are denoted as HT-d-r-333, HT-d-r-373, HT-d-r-423, HT-d-r-473, and HT-d-r-723, respectively.

A reference catalyst, $Mg(OH)_2$ (Sigma–Aldrich 99.9%), was activated by the same thermal decomposition and rehydration procedures described above for HT-d-r. The activated $Mg(OH)_2$ was then reheated to 373 K for 1 h in 100 $cm^3\,min^{-1}$ of N_2 to remove the physisorbed water before the reaction test. A reference MgO catalyst was prepared by thermal decomposition of the commercial $Mg(OH)_2$ using the same decomposition procedure as HT-d preparation.

2.2. Catalyst characterization

The weight loading of Mg and Al, and the trace analysis of Na were determined by ICP analysis (Galbraith Laboratories, Knoxville, TN). Dinitrogen adsorption isotherms were measured at 77 K using a Micromeritics ASAP 2020 and the surface area was calculated using the Brunauer–Emmett–Teller (BET) method. X-ray diffraction was performed on a Scintag XDS 2000 diffractometer using Cu$K\alpha$ radiation. Samples were scanned continuously over 2θ from 7° to 72° at a scan rate of 2° min^{-1}.

Thermogravimetric analysis (TGA) of HT and HT-d-r was performed on a TGA 2050 Thermogravimetric Analyzer (TA Instruments). Approximately 30 mg HT was used and the temperature was first ramped to 723 K at 2 $K\,min^{-1}$ and maintained at 723 K for 8 h under 100 $cm^3\,min^{-1}$ N_2; then the temperature was lowered to 298 K under 100 $cm^3\,min^{-1}$ N_2; rehydration was performed by flowing 100 $cm^3\,min^{-1}$ wet N_2 (2.6 vol% H_2O) at 298 K for 24 h; finally, thermogravimetric analysis was performed by ramping the temperature to 723 K at 2 $K\,min^{-1}$ in 100 $cm^3\,min^{-1}$ of flowing N_2.

The adsorption of CO_2 was performed on the TGA instrument. Approximately 30 mg HT was loaded for each analysis. The samples HT-d, HT-d-r, HT-d-r-333, HT-d-r-373, HT-d-r-423, HT-d-r-473 and HT-d-r-723 were prepared in situ in the TGA instrument using the same catalyst activation procedures, except the rehydration was performed at 298 K. Before CO_2 adsorption, HT-d-r was purged with 100 $cm^3\,min^{-1}$ N_2 at 298 K for 5 h to remove the physisorbed water. The CO_2 adsorption was performed with 100 $cm^3\,min^{-1}$ flowing CO_2 (Messer, 99.999%) at 298 K under atmospheric pressure for 1 h. Afterwards, the sample was purged with 100 $cm^3\,min^{-1}$ flowing N_2 for 1 h to remove weakly adsorbed CO_2.

2.3. Transesterification reaction

The transesterification reactions were performed at 333 K in a 500 ml glass batch reactor equipped with a condenser to reflux the methanol, stirred with a semicircular impeller (19 × 60 mm) at 180 rpm and purged with N_2 flowing at 40 $cm^3\,min^{-1}$. For each reaction, 136.5 g methanol (Fisher, 99.9%), 43.8 g tributyrin (Acros, 98%) and 6.5 g butyl ether (Sigma–Aldrich, 99.3%) used as an internal standard were charged to the reactor. In general, 0.25 g HT or $Mg(OH)_2$ was pretreated and moved

into the batch reactor without exposure to air to prevent CO_2 contamination of the base sites. Liquid samples were periodically removed and filtered for analysis. Analysis was performed on an HP 5890 Series II Gas Chromatograph equipped with a DB1 capillary column (30 m × 0.32 mm × 0.25 μm) and a flame ionization detector. The response factors for tributyrin, dibutyrin, monobutyrin and methyl butyrate were determined through multipoint calibrations of standards.

2.4. Kinetic modeling of transesterification

The transesterification of tributyrin (T) with methanol (M) can be described in three sequential steps: (1) tributyrin reacts with methanol to produce dibutyrin (D) and methyl butyrate (MB); (2) dibutyrin reacts further with methanol to produce monobutyrin (Mo) and methyl butyrate; (3) monobutyrin reacts with methanol to produce glycerol (G) and methyl butyrate. These three steps can be expressed in the following three reaction equations:

$$\mathrm{T} + \mathrm{M} \xrightarrow{k_1} \mathrm{D} + \mathrm{MB}, \tag{1}$$

$$\mathrm{D} + \mathrm{M} \xrightarrow{k_2} \mathrm{Mo} + \mathrm{MB}, \tag{2}$$

$$\mathrm{Mo} + \mathrm{M} \xrightarrow{k_3} \mathrm{G} + \mathrm{MB}. \tag{3}$$

Although each step of the transesterification reaction is reversible, Diasakou et al. proposed that the reverse reactions in excess methanol were not important and could be ignored [20]. Each step of the reaction was assumed to be first order to each reaction component [20–23]. In this study, all the reactions were carried out with a methanol:tributyrin molar ratio of 30:1. With such a large excess of methanol, we further assumed pseudo first order kinetics with respect to the butyrin components. Our kinetic analysis also attempted to quantify the deactivation rate. The same empirical exponential deactivation component, $\exp(-\alpha t)$, was applied for all three reactions, where α is deactivation parameter (min^{-1}), and t is reaction time (min). The normalized moles for T, D, Mo, G and MB are defined as $y_i = [i]/[\mathrm{T}]_0$, where i = T, D, Mo, or G, and $y_{\mathrm{MB}} = [\mathrm{MB}]/[\mathrm{T}]_0/3$. In these expressions, $[i]$ is the concentration of species i ($\mathrm{mol\,L}^{-1}$) and $[\mathrm{T}]_0$ is the initial concentration of tributyrin ($\mathrm{mol\,L}^{-1}$). In this way, $1 - y_{\mathrm{T}}$ will be the conversion of tributyrin and y_i will be the yield of species i, where i = MB, D, Mo, or G.

Based on the above reaction mechanism and assumptions, the differential equations describing the reaction system are:

$$\frac{dy_{\mathrm{T}}}{dt} = -S[\mathrm{M}]_0 k_1 y_{\mathrm{T}} e^{-\alpha t}, \tag{4}$$

$$\frac{dy_{\mathrm{D}}}{dt} = S[\mathrm{M}]_0 (k_1 y_{\mathrm{T}} - k_2 y_{\mathrm{D}}) e^{-\alpha t}, \tag{5}$$

$$\frac{dy_{\mathrm{Mo}}}{dt} = S[\mathrm{M}]_0 (k_2 y_{\mathrm{D}} - k_3 y_{\mathrm{Mo}}) e^{-\alpha t}, \tag{6}$$

$$\frac{dy_{\mathrm{G}}}{dt} = S[\mathrm{M}]_0 k_3 y_{\mathrm{Mo}} e^{-\alpha t}, \tag{7}$$

$$3\frac{dy_{\mathrm{MB}}}{dt} = S[\mathrm{M}]_0 (k_1 y_{\mathrm{T}} + k_2 y_{\mathrm{D}} + k_3 y_{\mathrm{Mo}}) e^{-\alpha t}, \tag{8}$$

Table 1
Surface area of activated HT and reference catalysts

Sample	BET surface area ($\mathrm{m^2\,g^{-1}}$)
HT-d	265
HT-d-r	40
HT-d-r-333	41
HT-d-r-373	43
HT-d-r-423	44
HT-d-r-473	47
MgO[a]	22
$Mg(OH)_2$[b]	17

[a] MgO was prepared by decomposing the commercial $Mg(OH)_2$ at 723 K for 8 h in 100 $\mathrm{cm^3\,min^{-1}}$ flowing N_2.

[b] $Mg(OH)_2$ was prepared by rehydrating the decomposed commercial $Mg(OH)_2$ at room temperature for 24 h in 100 $\mathrm{cm^3\,min^{-1}}$ wet N_2 (2.6 vol% H_2O) flow and then heating at 373 K for 1 h in 100 $\mathrm{cm^3\,min^{-1}}$ flowing N_2.

where k_1, k_2, and k_3 are reaction constants normalized per unit catalyst surface area for the three transesterification reaction steps ($\mathrm{mol^{-1}\,L\,m^{-2}\,min^{-1}}$); S is total surface area of catalyst ($\mathrm{m^2}$); and $[\mathrm{M}]_0$ is the initial concentration of methanol ($\mathrm{mol\,L^{-1}}$). The MATLAB function ode45 was applied to solve the differential equations and another MATLAB function lsqcurvefit was used to minimize the value of $\sum_i \sum_t (y_{i,t,\mathrm{cal}} - y_{i,t,\mathrm{exp}})^2$ to estimate the rate constants and deactivation parameters, where the index i runs through T, D, Mo, G, and MB and the index t runs through the experimental data points. The subscripts cal and exp refer to the calculated value and experimental value, respectively. The MATLAB function nlparci was applied to estimate the 95% confidence intervals of the rate constants and deactivation parameters.

3. Results and discussion

The elemental analysis and the TGA results indicated the composition of the synthesized Mg–Al hydrotalcite was $[Mg_{0.795}Al_{0.205}(OH)_2]^{0.205+}(CO_3)^{2-}_{0.1025}\cdot 0.88H_2O$ with a trace amount of Na at 62 ppm. The effect of the small amount of Na on catalysis was neglected. The Mg/Al molar ratio was close to the nominal ratio of 4:1. The BET surface areas listed in Table 1 revealed that HT-d had a very high surface area of 265 $\mathrm{m^2\,g^{-1}}$ compared to the rehydrated sample, HT-d-r, 40 $\mathrm{m^2\,g^{-1}}$. The surface areas of thermally treated HT-d-r at temperatures from 333 to 473 K remained relatively constant, presumably because the layered structure remained intact at these modest temperatures.

Results from thermogravimetric analysis (TGA) and differential thermogravimetric analysis (DTA) of HT are shown in Fig. 1. The DTA curve shows two main weight loss features from dehydration and decomposition. The loss by dehydration, which occurs below 473 K, is attributed to the removal of interlayer water [24–26]. The decomposition of these layers, which occurs above 473 K, leads to the formation of high surface area mixed oxides. This process is the result of simultaneous decarbonation of the interlayer carbonate anions and dehydroxylation of the brucite-like layers.

Fig. 2 illustrates the TGA and DTA curves for a HT-d-r sample. Three weight loss peaks appear on the DTA curve of

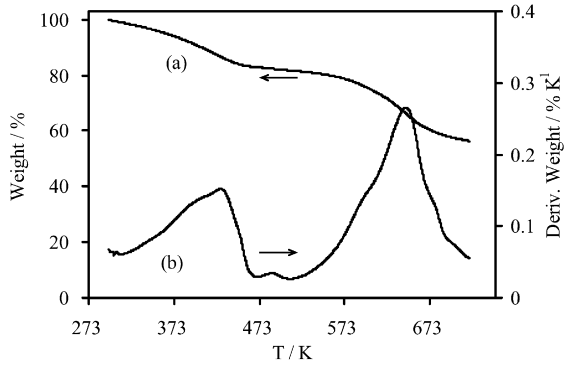

Fig. 1. (a) Thermogravimetric analysis (TGA), (b) differential thermogravimetric analysis (DTA) for HT.

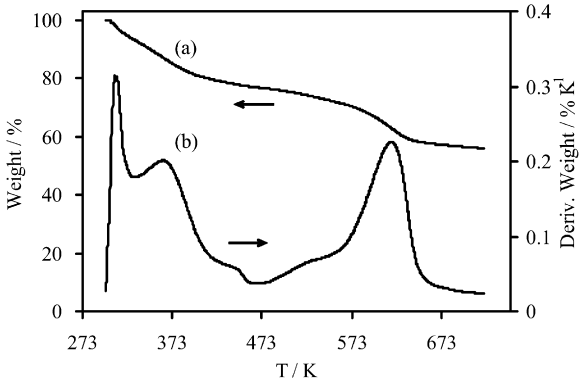

Fig. 2. (a) Thermogravimetric analysis (TGA), (b) differential thermogravimetric analysis (DTA) for HT-d-r.

HT-d-r. The first two peaks appearing at 313 and 363 K are attributed to the removal of physisorbed water and interlayer water, respectively. The dehydration of interlayer water happens in a broad temperature range from 333 to 473 K. The decomposition of the sample occurs above 473 K and is attributed to the simultaneous dehydroxylation of the charge-balancing interlayer hydroxyl anions and the brucite-like layers.

The X-ray diffraction (XRD) patterns of HT, HT-d, HT-d-r, and various thermally-treated HT-d-r samples are presented in Fig. 3. The XRD pattern of the synthesized hydrotalcite (HT) has the typical reflections associated with the double layered hydroxide. After decomposition at 723 K for 8 h, the layered structure of HT disappeared and the mixed oxide with high surface area was formed. The original hydrotalcite layered structure was essentially reformed by a stream of humidified N_2 over the decomposed HT at room temperature for 24 h. However, the crystallinity of HT-d-r decreased upon dehydration from 333 to 473 K, which is characteristic of dehydration of Mg–Al hydrotalcite [27]. The intensity of the (003) peak at $2\theta = 11.2°$ and the (006) peak at $2\theta = 22.4°$, which are associated with the interlayer spacing, decreased and the peak width increased as the treatment temperature increased. At 423 and 473 K the (006) reflections were almost absent.

The transesterification of tributyrin with methanol over activated Mg–Al hydrotalcite catalysts was then performed. The possible products from the three step reaction sequence are methyl butyrate, dibutyrin, monobutyrin and glycerol. The initial reaction rate of tributyrin over HT-d-r was proportional to the catalyst weight loading in the range of 0.125–1.0 g. The Weisz modulus [28], $\Phi = (r_T \rho_s)_{obs} R^2 / D_{eff}[T]$, where r_T is the reaction rate of tributyrin (8.0×10^{-5} mol s^{-1} g^{-1}), ρ_s is the catalyst particle density (2 g cm^{-3}), R is the catalyst particle radius (0.038 mm), D_{eff} is the effective diffusion coefficient (10^{-5} cm^2 s^{-1}), and [T] is the tributyrin concentration (0.7 mol L^{-1}), was used to evaluate the effect of internal diffusion. The Weisz modulus Φ was estimated to be 0.3, which was similar to the Weisz modulus $\Phi = 0.2$ reported by Rao et al. for the condensation of benzaldehyde with acetone over rehydrated hydrotalcite [16]. The Weisz modulus of 0.3 corresponds to an effectiveness factor greater than 0.95 and thus the effects of mass transfer were neglected in the reporting of observed rates.

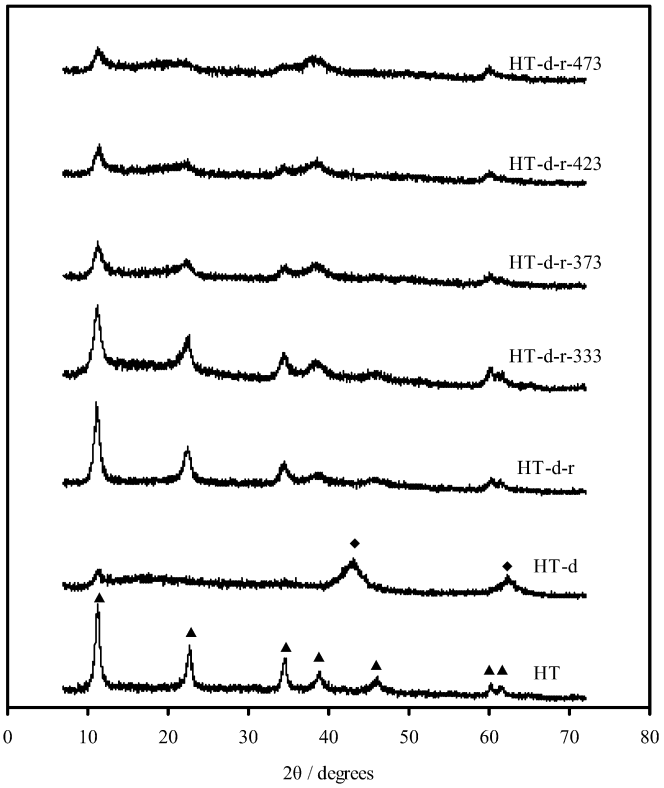

Fig. 3. X-ray diffraction patterns of HT, HT-d, HT-d-r, HT-d-r-333, HT-d-r-373, HT-d-r-423, and HT-d-r-473. (▲) Hydrotalcite, (◆) MgO.

To check for leaching of catalyst into the reaction medium, HT-d-r catalyst was removed from the reactor after 100 min of reaction. As illustrated by the reaction profile in Fig. 4, the conversion of tributyrin was abruptly stopped after removal of the catalyst at 100 min. Moreover, the composition of the products did not change after filtering. These results confirm that catalysis was associated with the solid phase material.

Typical reaction profiles over HT-d, HT-d-r, HT-d-r-373, and HT-d-r-473 are illustrated in Fig. 5. The solid curves show the results of fitting the three step reaction sequence to the kinetic data. The reaction rate constants and deactivation parameters associated with those curves are listed in Table 2. The rehydrated sample (HT-d-r) had the highest catalytic activity on both a weight and surface area basis, reaching over 80% tribu-

tyrin conversion and nearly 80% yield to methyl butyrate within 400 min. The reaction rate constant (surface area basis) of the first transesterification reaction step on HT-d-r was one order of magnitude greater than that of HT-d. The reference MgO catalyst should also have strong Lewis base sites like HT-d, whereas $Mg(OH)_2$ has the brucite layered structure without the Brønsted base sites associated with HT-d-r. The rate constant k_1 over MgO was about 3 times greater than that over HT-d (Table 2), probably because of the higher base site density of MgO [29]. Nevertheless, the rate constant was still significantly lower than that associated with the rehydrated sample, HT-d-r.

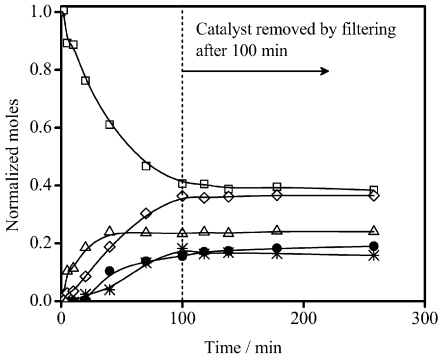

Fig. 4. Leaching test of HT-d-r for transesterification of tributyrin with methanol. Reaction conditions: methanol 136.5 g, tributyrin 43.0 g, 0.25 g HT, and 333 K. (◇) Methyl butyrate, (□) tributyrin, (△) dibutyrin, (●) monobutyrin, (∗) glycerol (calculated by the mass balance between methyl butyrate, dibutyrin, monobutyrin, and glycerol, $y_G = (3y_{MB} - y_D - 2y_{Mo})/3$). Curves were drawn to guide the eye.

Table 2
Reaction rate constants and deactivation parameters from transesterification of tributyrin with methanol

Catalyst	k_1[a] ($\times 10^6$)	k_2[a] ($\times 10^6$)	k_3[a] ($\times 10^6$)	α[b]
HT-d	2.5± 0.2	3.1 ± 0.4	–	(8.6 ± 1.8) × 10^{-4}
HT-d-r	50 ± 2	132 ± 14	120 ± 14	(3.8 ± 0.2) × 10^{-3}
HT-d-r-333	46 ± 2	110 ± 12	110 ± 16	(2.9 ± 0.2) × 10^{-3}
HT-d-r-373	11 ± 1	16 ± 2	–	(1.7 ± 0.2) × 10^{-3}
HT-d-r-423	1.7 ± 0.4	–	–	–
HT-d-r-473	0.21 ± 0.2	–	–	–
HT-d-r-723	1.7 ± 0.2[c]	2.0 ± 0.5[c]	–	(5.7 ± 2.6) × 10^{-4}
MgO[d]	7.4 ± 1.5	9.2 ± 3.7	–	–
$Mg(OH)_2$[e]	1.7 ± 1.7	–	–	–
HT-d-r-T[f]	13 ± 1.6	14 ± 3	–	(3.4 ± 0.6) × 10^{-3}
HT-d-r-M[g]	44 ± 3	100 ± 13	242 ± 67	(6.3 ± 0.5) × 10^{-3}

[a] Reaction rate constant with 95% confidence interval (L mol^{-1} m^{-2} min^{-1}).
[b] Deactivation parameter with 95% confidence interval (min^{-1}).
[c] Sample treated as having same surface area as HT-d.
[d] MgO was prepared by decomposing the commercial $Mg(OH)_2$ at 723 K for 8 h in 100 cm^3 min^{-1} flowing N_2.
[e] $Mg(OH)_2$ was prepared by rehydrating the decomposed commercial $Mg(OH)_2$ at room temperature for 24 h in 100 cm^3 min^{-1} wet N_2 (2.6 vol% H_2O) flow and then heating at 373 K for 1 h in 100 cm^3 min^{-1} flowing N_2.
[f] Pretreatment of HT-d-r with tributyrin for 1 h at 333 K.
[g] Pretreatment of HT-d-r with methanol for 1 h at 333 K.

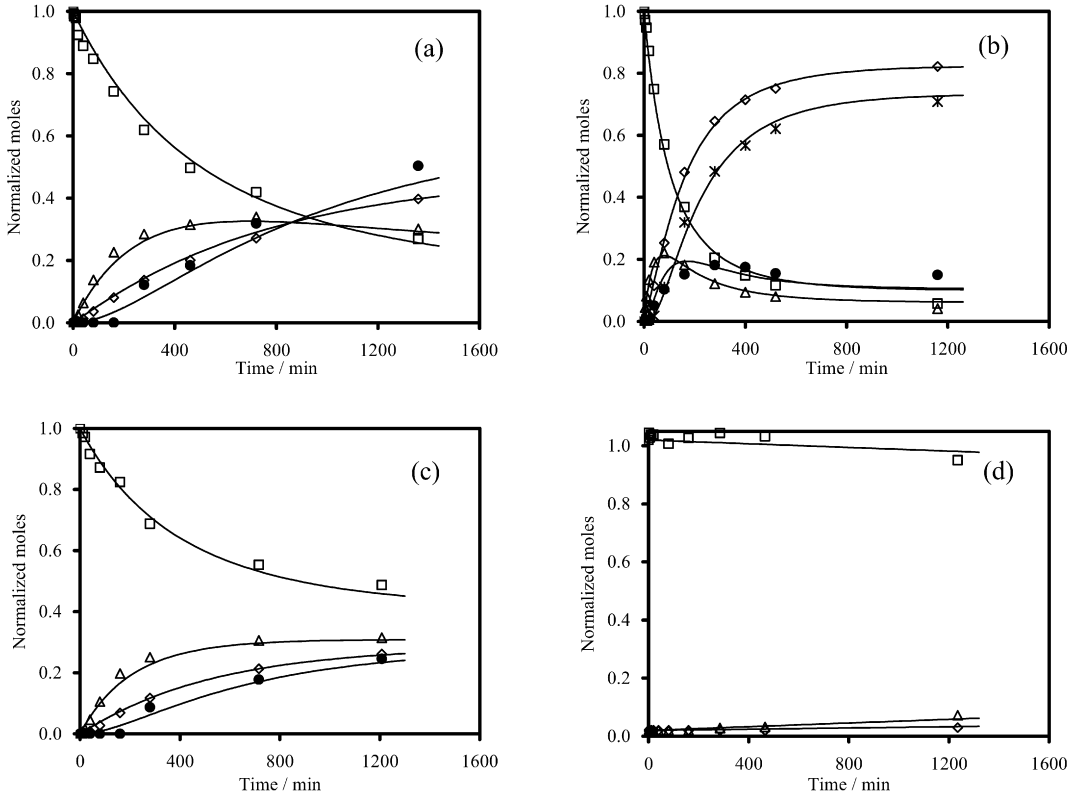

Fig. 5. Reaction profiles of transesterification of tributyrin with methanol catalyzed by 0.25 g HT activated under different conditions: (a) HT-d, (b) HT-d-r, (c) HT-d-r-373, (d) HT-d-r-473. Reaction conditions: methanol 136.5 g, tributyrin 43.0 g, and 333 K. (◇) Methyl butyrate, (□) tributyrin, (△) dibutyrin, (●) monobutyrin, (∗) glycerol (calculated by the mass balance between methyl butyrate, dibutyrin, monobutyrin, and glycerol, $y_G = (3y_{MB} - y_D - 2y_{Mo})/3$). The solid curves represent the calculated profiles, using the parameters in Table 2.

The catalytic activity of $Mg(OH)_2$ was also much lower than that of HT-d-r. From the comparison of activity between the two reference catalysts, HT-d and HT-d-r, we conclude that the charge-balancing hydroxyl anions, i.e., the Brønsted base sites, are the active sites for the transesterification reaction; the hydroxyl groups coordinated to Mg and Al in the brucite-like layers of HT-d-r have negligible catalytic activity compared to the Brønsted base sites.

Removing the physisorbed molecular water of HT-d-r by heating to 333 K for 1 h (producing HT-d-r-333) did not significantly alter the catalytic activity. However, upon removal of interlayer water at temperatures above 333 K, the catalytic activity decreased substantially. Heating HT-d-r to 473 K apparently removed all the interlayer water (according to TGA) and resulted in a significant loss of Brønsted basicity, as illustrated by the very poor catalytic activity of this sample (Fig. 5d). When HT-d-r was heated to the decomposition temperature of 723 K for 1 h, the mixed Mg–Al oxide exposing Lewis base sites was recovered.

The catalyst exhibiting the highest reaction rate constants also contained the most adsorbed water and deactivated faster (Table 2). The relatively low deactivation rate of HT-d and HT-d-r-723 might be due to the retained organic compounds on these materials [12]. It should be mentioned that ignoring the effect of the reverse reactions at high conversion can result in a higher fitted deactivation parameter. However, butyric acid from the hydrolysis of ester in the presence of adsorbed water would also poison the base sites on the catalysts. The same deactivation mechanism has been pointed out by Corma et al. [12]. Similarly, Shibasaki-Kitakawa et al. indicated that the deactivation of anion-exchange resin (PA306s) for transesterification of triolein with ethanol was due to a direct exchange of hydroxyl with oleate [30]. To test for deactivation in our system, the HT-d-r catalyst was stirred with tributyrin for 1 h at 333 K, denoted as HT-d-r-T, before adding methanol to perform the reaction. For comparison HT-d-r catalyst was stirred with methanol for 1 h at 333 K, denoted as HT-d-r-M, before adding tributyrin to perform the reaction. The reaction rate constants and deactivation parameters for HT-d-r-T and HT-d-r-M are listed in Table 2. The tributyrin pretreatment of HT-d-r significantly decreased its activity. The reaction rate constant k_1 decreased by a factor of 4 and k_2 decreased by a factor of 10 as a result of tributyrin pretreatment whereas the catalytic activity of HT-d-r pretreated with methanol did not change significantly. Apparently, hydrolysis of the ester led to catalyst deactivation. However, the presence of water on the sample also appeared to be crucial for high catalytic activity.

Researchers have proposed that only a small number of Brønsted base sites located at the edges of the hydrotalcite platelets are the active base sites for catalysis [17,31–35]. In many of these studies, adsorption of CO_2 at low pressure was used to count the base sites located on the crystallite edges. In our work, we adsorbed CO_2 at atmospheric pressure in the TGA. The amount of adsorbed CO_2 normalized by catalyst surface area is plotted versus treatment temperature in Fig. 6. From the CO_2 uptake over HT-d-r sample and assuming one CO_2 molecule adsorbed on one base site, we calculate that 41% of

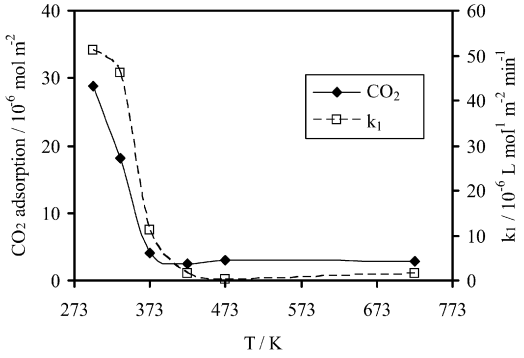

Fig. 6. CO_2 adsorption capacity (measured at atmospheric pressure of CO_2) and transesterification reaction rate constant k_1 of HT-d-r during thermal treatment at temperature ranging from 298 to 723 K.

the charge-balancing hydroxyl groups reacted with CO_2, which is much higher than the uptakes reported by others using adsorption of CO_2 at low pressure (∼mbar) [17,31–35]. In fact, Abello et al. titrated 30% of the base sites only when the surface area of a rehydrated sample was about 270 $m^2\,g^{-1}$, which far exceeds the surface area of our rehydrated materials [17]. Based on the surface area of the HT-d-r sample, we estimate that less than 10% of the hydroxyl groups were present on the external catalyst surface. Evidently, exposure of the sample to CO_2 at atmospheric pressure allowed for hydroxyl groups on the external surfaces as well as many located between the layers to be titrated.

The corresponding reaction rate constant k_1 for various temperature treatments is also plotted in Fig. 6. The CO_2 adsorption capacity and reaction rate constant k_1 for the samples are well correlated. At temperatures below 473 K, HT-d-r undergoes a dehydration process without significantly decreasing the surface area (Table 1). However, the CO_2 adsorption capacity decreased significantly upon heating, reaching a minimum at 423 K, and then increased slightly when heated to 473 K. This slight increase was likely the result of the partial decomposition of the hydroxyl groups in the brucite-like layers. The in situ DRIFTS study by Yang et al. shows that the hydroxyl groups bonded to Al cations in the layers begin disappearing at 463 K in the case of Mg–Al–CO_3 hydrotalcite [36]. Moreover, the Mg and Al K-edge XAFS study by van Bokhoven et al. indicates that the dehydroxylation of Mg–Al hydrotalcite commences between 425 and 473 K [37]. The HT-d-r sample with hydroxyl as the interlayer anion is probably less stable than a hydrotalcite sample with carbonate as the interlayer anion since hydrotalcites containing less basic anions are proposed to be more thermally stable [38]. The partial decomposition of the brucite-like layers could lead to the formation of weak Lewis base sites associated with Al–O groups on the surface. Thermal treatment up to 473 K decreased the observed catalytic activity for transesterification. The loss of active Brønsted base sites could result from the increasing interaction between the interlayer hydroxyl anions and the brucite-like layer as the interlayer water is gradually removed. Based on the powder XRD and ^{27}Al MAS-NMR experiments performed on Mg–Al hydrotalcite (Mg/Al = 2.0) sample heated to 473 K, Bellotto et al. propose that Al atoms diffuse out of the octahedral sites of the

Table 3
Turnover frequency of transesterification of tributyrin with methanol based on CO_2 uptake

Catalyst	Obs. TOF[a] (s^{-1})	TOF_{k1}[b] (s^{-1})
HT-d	0.065	0.051
HT-d-r	0.057	0.081
HT-d-r-333	0.074	0.12
HT-d-r-373	0.15	0.12
HT-d-r-423	0.032	0.031
HT-d-r-473	0.0037	0.0031
HT-d-r-723	0.018	0.027

[a] Based on initial conversion of tributyrin, normalized by CO_2 uptake.
[b] Based on the rate constant k_1 in Table 2, normalized by CO_2 uptake.

brucite-like layers and coordinate tetrahedrally to both the layer and the interlayer oxygens [39]. The in situ DRIFTS study by Yang et al. also indicates an increasing interaction between interlayer carbonate anion and the Mg–Al hydrotalcite layer during interlayer water removal [36]. As HT-d-r was decomposed between 473 and 723 K, the CO_2 adsorption capacity remained fairly constant as shown in Fig. 6, and was similar to the CO_2 adsorption capacity of HT-d (2.2×10^{-6} mol m^{-2}).

Based on CO_2 uptake, the turnover frequencies (TOF) of transesterification of tributyrin with methanol over activated HT were calculated and listed in Table 3. The observed TOF values (obs. TOF) based on initial rate of consumption of tributyrin are similar to those derived from the fitted values of k_1 (TOF_{k1}). The TOF values of HT-d-r sample and its thermally-treated samples up to 373 K remained relatively constant and then decreased significantly when heated to 473 K, probably due to the loss of the Brønsted base sites upon heating and formation of weak Lewis base sites upon partially decomposition of the layered structure. There is no significant difference between TOF values of the Brønsted base sites of HT-d-r sample and that of the Lewis base sites of HT-d sample. If the Brønsted base sites located on the crystallite edges are the active sites for the rehydrated sample, then the true turnover frequencies of the Brønsted base catalysts are much greater than the values reported here. However it has been observed that the transesterification of 5-carboxyfluorescein with 1-butanol over [Li^+–Al^{3+}] layered double hydroxide catalyst occurs on the basal planes of the crystal surface without the preference for crystal edges [40]. Moreover, we cannot exclude the possibility that hydroxyl groups in the rehydrated layers are participating in the observed catalysis. The presence of water in the interlayer regions may allow methanol to penetrate into the interlayer regions or may increase the mobility of the interlayer hydroxyl groups.

4. Conclusions

A hydrotalcite material with a Mg/Al molar ratio of 4 was successfully synthesized by a coprecipitation method. The hydrotalcite sample that was decomposed by a thermal treatment at 723 K could be reconstructed by vapor phase rehydration, and the crystallinity of the rehydrated sample decreased during additional thermal treatments at temperatures below 473 K. The fitted reaction rate constants for the transesterification of tributyrin with excess methanol quantitatively described the catalytic activity of the activated Mg–Al hydrotalcite. The decomposed-rehydrated sample, having Brønsted base sites residing on and between the brucite-like layers was an order of magnitude more active on a surface area basis than a decomposed sample which exposed Lewis base sites. However, the TOF values of the HT-d-r and HT-d samples do not show a significant difference when normalized by the CO_2 adsorption capacity. Heating a rehydrated sample to 473 K caused a loss in both activity and CO_2 adsorption capacity, thus suggesting water management on HT-d-r is crucial for effective catalysis. Brønsted base sites were active in the presence of water, but high levels of hydration caused rapid deactivation of the catalyst, presumably by ester hydrolysis to butyric acid that reacted with the base sites.

Acknowledgments

This work was supported by the Chemical Sciences, Geosciences and Biosciences Division, Office of Basic Energy Sciences, Office of Science, U.S. Department of Energy, grant No. DE-FG02-95ER14549.

References

[1] J. Van Gerpen, Fuel Process. Technol. 86 (2005) 1097.
[2] F.R. Ma, M.A. Hanna, Biores. Technol. 70 (1999) 1.
[3] L.C. Meher, D.V. Sagar, S.N. Naik, Renew. Sust. Energ. Rev. 10 (2006) 248.
[4] A.C. Pinto, L.L.N. Guarieiro, M.J.C. Rezende, N.M. Ribeiro, E.A. Torres, W.A. Lopes, P.A.D. Pereira, J.B. de Andrade, J. Brazil. Chem. Soc. 16 (2005) 1313.
[5] G. Vicente, M. Martinez, J. Aracil, Biores. Technol. 92 (2004) 297.
[6] T. Ebiura, T. Echizen, A. Ishikawa, K. Murai, T. Baba, Appl. Catal. A Gen. 283 (2005) 111.
[7] R. Stern, G. Hillion, J.J. Rouxel, S. Leporq, U.S. patent 5 908 946 (1999) to Institut Francais du Petrole.
[8] G.J. Suppes, M.A. Dasari, E.J. Doskocil, P.J. Mankidy, M.J. Goff, Appl. Catal. A Gen. 257 (2004) 213.
[9] D.E. Lopez, J.G. Goodwin, D.A. Bruce, E. Lotero, Appl. Catal. A Gen. 295 (2005) 97.
[10] M. Di Serio, M. Ledda, M. Cozzolino, G. Minutillo, R. Tesser, E. Santacesaria, Ind. Eng. Chem. Res. 45 (2006) 3009.
[11] F. Cavani, F. Trifiro, A. Vaccari, Catal. Today 11 (1991) 173.
[12] A. Corma, S.B. Abd Hamid, S. Iborra, A. Velty, J. Catal. 234 (2005) 340.
[13] B.F. Sels, D.E. De Vos, P.A. Jacobs, Catal. Rev. 43 (2001) 443.
[14] A.L. McKenzie, C.T. Fishel, R.J. Davis, J. Catal. 138 (1992) 547.
[15] J.I. Di Cosimo, V.K. Diez, M. Xu, E. Iglesia, C.R. Apesteguia, J. Catal. 178 (1998) 499.
[16] K.K. Rao, M. Gravelle, J.S. Valente, F. Figueras, J. Catal. 173 (1998) 115.
[17] S. Abello, F. Medina, D. Tichit, J. Perez-Ramirez, J.C. Groen, J.E. Sueiras, P. Salagre, Y. Cesteros, Chem. Eur. J. 11 (2005) 728.
[18] B.M. Choudary, M.L. Kantam, C.R.V. Reddy, K.K. Rao, F. Figueras, J. Mol. Catal. A Chem. 146 (1999) 279.
[19] D.G. Cantrell, L.J. Gillie, A.F. Lee, K. Wilson, Appl. Catal. A Gen. 287 (2005) 183.
[20] M. Diasakou, A. Louloudi, N. Papayannakos, Fuel 77 (1998) 1297.
[21] H. Noureddini, D. Zhu, J. Am. Oil Chem. Soc. 74 (1997) 1457.
[22] S.K. Karmee, D. Chandna, R. Ravi, A. Chadha, J. Am. Oil Chem. Soc. 83 (2006) 873.
[23] B. Freedman, R.O. Butterfield, E.H. Pryde, J. Am. Oil Chem. Soc. 63 (1986) 1375.
[24] J. Rocha, M. del Arco, V. Rives, M.A. Ulibarri, J. Mater. Chem. 9 (1999) 2499.

[25] D. Tichit, M.N. Bennani, F. Figueras, J.R. Ruiz, Langmuir 14 (1998) 2086.
[26] D. Tichit, M.H. Lhouty, A. Guida, B.H. Chiche, F. Figueras, A. Auroux, D. Bartalini, E. Garrone, J. Catal. 151 (1995) 50.
[27] J. Perez-Ramirez, S. Abello, N.M. van der Pers, Chem. Eur. J. 13 (2007) 870.
[28] P.B. Weisz, Adv. Catal. 13 (1962) 137.
[29] C.T. Fishel, R.J. Davis, Catal. Lett. 25 (1994) 87.
[30] N. Shibasaki-Kitakawa, H. Honda, H. Kuribayashi, T. Toda, T. Fukumura, T. Yonemoto, Biores. Technol. 98 (2007) 416.
[31] J.C.A.A. Roelofs, A.J. van Dillen, K.P. de Jong, Catal. Today 60 (2000) 297.
[32] J.C.A.A. Roelofs, D.J. Lensveld, A.J. van Dillen, K.P. de Jong, J. Catal. 203 (2001) 184.
[33] F. Winter, A.J. van Dillen, K.P. de Jong, Chem. Commun. 31 (2005) 3977.
[34] F. Winter, V. Koot, A.J. van Dillen, J.W. Geus, K.P. de Jong, J. Catal. 236 (2005) 91.
[35] F. Winter, X.Y. Xia, B.P.C. Hereijgers, J.H. Bitter, A.J. van Dillen, M. Muhler, K.P. de Jong, J. Phys. Chem. B 110 (2006) 9211.
[36] W.S. Yang, Y. Kim, P.K.T. Liu, M. Sahimi, T.T. Tsotsis, Chem. Eng. Sci. 57 (2002) 2945.
[37] J.A. van Bokhoven, J.C.A.A. Roelofs, K.P. de Jong, D.C. Koningsberger, Chem. Eur. J. 7 (2001) 1258.
[38] J.C.A.A. Roelofs, J.A. van Bokhoven, A.J. van Dillen, J.W. Geus, K.P. de Jong, Chem. Eur. J. 8 (2002) 5571.
[39] M. Bellotto, B. Rebours, O. Clause, J. Lynch, D. Bazin, E. Elkaim, J. Phys. Chem. 100 (1996) 8535.
[40] M.B.J. Roeffaers, B.F. Sels, H. Uji-i, F.C. De Schryver, P.A. Jacobs, D.E. De Vos, J. Hofkens, Nature 439 (2006) 572.